



Published in final edited form as:

Ophthalmic Surg Lasers Imaging. 2011 July ; 42(0): S56–S66. doi:10.3928/15428877-20110627-05.

The Role of Spectral-Domain OCT in the Diagnosis and Management of Neovascular Age-Related Macular Degeneration

Caio V. Regatieri, MD, PhD, Lauren Branchini, BA, and Jay S. Duker, MD

New England Eye Center (CVR, LB, JSD), Tufts Medical Center, Boston, Massachusetts; the Department of Ophthalmology (CVR), Federal University of São Paulo, São Paulo, Brazil; and Boston University School of Medicine (LB), Boston, Massachusetts

Abstract

Spectral-domain optical coherence tomography (SD-OCT) has emerged as the ancillary examination of choice to assist the diagnosis and management of neovascular age-related macular degeneration (AMD). SD-OCT provides more detailed images of intraretinal, subretinal, and subretinal pigment epithelium fluid when compared to time-domain technology, leading to higher and earlier detection rates of neovascular AMD activity. Improvements in image analysis and acquisition speed make it important for decision-making in the diagnosis and treatment of this disease. However, this new technology needs to be validated for its role in the improvement of visual outcomes in the context of anti-angiogenic therapy.

INTRODUCTION

Age-related macular degeneration (AMD) is the leading cause of severe visual loss in adults older than 60 years.^{1,2} It is estimated that approximately 30% of adults older than 75 years have some sign of AMD and approximately 10% develop advanced stages of the disease. More than 1.6 million people in the United States currently have one or both eyes affected by an advanced stage of AMD and it is estimated that there are another 7 million individuals “at risk.”¹ Due to rapid aging of the population in many developed countries, this number is expected to double by the year 2020.^{1,3} Although neovascular AMD only accounts for approximately 10% to 20% of the overall AMD incidence, this sub-type is responsible for 90% of cases of severe vision loss (visual acuity of 20/200 or worse).^{4,5}

Neovascular AMD is characterized by the presence of choroidal neovascularization (CNV) and is associated with retinal pigment epithelium detachment (PED), retinal pigment epithelium (RPE) tears, fibrovascular disciform scarring, and vitreous hemorrhage.⁴ Neovascularization may be predominantly within the retina. This is known as retinal angiomatous proliferation.⁶

Historically, neovascularization associated with AMD has been classified several ways. These classifications have been driven by both the technology available to detect neovascularization and the therapeutic options available. Fluorescein angiography, which allows functional assessment of neovascularization, was used to develop a classification scheme within the context of photodynamic therapy.^{7,8} Because photodynamic therapy is a localized therapy, lesions were classified into “classic” early well-demarcated choroidal

Copyright © SLACK Incorporated

Address correspondence to Jay S. Duker, MD, New England Eye Center, Tufts Medical Center, 800 Washington Street, Boston, MA 02111. Jduker@tuftsmedicalcenter.org.

The remaining authors have no financial or proprietary interest in the materials presented herein.

hyperfluorescence with progressive pooling of dye leakage in the later phases on fluorescein angiography or “occult” poorly defined lesions on fluorescein angiography that may be accompanied by mottled hyperfluorescence in the mid-phase with associated late leakage or as late leakage of undetermined origin.^{7,9,10}

Additionally, the advent of indocyanine green angiography helped to detect and better define the borders of more neovascular membranes.¹¹ Indocyanine green angiography also defined another type of neovascularization, known as type 3 or retinal angiomatous proliferation, which is an intraretinal neovascularization.^{11,12}

Using both biomicroscopic criteria and fluorescein angiography, Gass proposed a classification of CNV based on the location of the neovascular complex with respect to the RPE layer. Lesions are classified as type 1 when the vessels are confined under the RPE or type 2 when the vessels proliferate in the subretinal space.¹³ Histopathologic investigation of specimens from submacular surgery demonstrates that CNV due to AMD is more likely to be below the RPE than CNV from other causes.¹⁴ As such, this kind of classification was useful in predicting outcomes of submacular surgery.

Until recently, fluorescein angiography was the primary imaging modality used to detect the presence and activity of CNV. Although fluorescein angiography is useful for determining presence of leakage in neovascular AMD, this technique does not provide any three-dimensional anatomic information about retinal layers, the RPE, or the choroid. The development of optical coherence tomography (OCT) makes it possible to have cross-sectional images of the macula or optic nerve head analogous to ultrasonography.

Because OCT represents a new imaging modality, a more refined classification of neovascularization has been proposed by Freund et al. to employ multimodal imaging where use of fluorescein angiography and indocyanine green angiography guide the location of the OCT to acquire both functional and anatomic information about the lesion. In this classification, type 1 corresponds to neovascularization below the RPE monolayer, type 2 corresponds to neovascularization in the subretinal space, and type 3 corresponds to an intraretinal lesion.¹⁵

Instead of sound, OCT uses light waves to obtain a reflectivity profile of the tissue under investigation.¹⁶ Light from a broadband light source is divided into a reference beam traveling a delay path and a sample beam that is directed onto the subject's retina. Light backscattered by retinal structures interferes with light from the reference beam. The interference of echoes is detected to create a measurement of light echoes versus depth. Standard OCT systems such as the Stratus OCT (Carl Zeiss Meditec, Inc., Dublin, CA) use time-domain detection, in which the reference mirror position and delay are mechanically scanned to produce axial scans (A-scans) of light echoes versus depth. Scan rates of 400 A-scans per second with an axial resolution of 8 to 10 μm in the eye are achieved with the Stratus OCT.¹⁷ In cases with active neovascular AMD, OCT can be used to detect signs of activity and to establish a baseline retinal thickness, volume, and fluid involvement. Additionally, OCT is particularly helpful in identifying the location and level of CNV (intraretinal, subretinal, and subretinal pigment epithelium) and other lesion components (blood, fluid, pigment, and fibrosis).¹⁸ In cases suspicious for exudative changes, OCT can be extremely useful in detecting suspected intraretinal, subretinal, or subretinal pigment epithelium fluid, especially when angiographic interpretation is equivocal, inconvenient, or not readily accessible.^{19,20}

Spectral-domain OCT (SD-OCT) or Fourier-domain detection uses a high-speed spectrometer to measure light echoes from all time delays, simultaneously enhancing OCT capabilities. The reference mirror does not require mechanical scanning. Improved

sensitivity enables dramatic improvements in sampling speed and signal-to-noise ratio.^{21,22} SD-OCT detection, coupled with improvements in light sources, achieves axial scanning speeds of greater than 20,000 A-scans per second with an axial resolution of 3 to 7 μm in the eye (Fig. 1). Nine commercial SD-OCT or Fourier-domain OCT systems are currently available worldwide. SD-OCT has emerged as the ancillary examination of choice to assist the diagnosis and management of neovascular AMD. SD-OCT has the advantage of detecting small changes in the morphology of the retinal layers and subretinal space, allowing for precise anatomic detection of structural changes that may correspond to progression or regression of the neovascular lesions.^{23,24}

Several focal treatments have been proposed and extensively studied to prevent the severe visual loss in patients with neovascular AMD, including laser photocoagulation,⁹ photodynamic therapy,¹⁰ and the combination of photodynamic therapy with intraocular injections of triamcinolone acetonide. Despite anatomical success, there is a low chance for visual improvement when these treatments are used. In recent years, research has provided new insights into the pathogenesis of macular disease. Less destructive treatments directly targeting CNV and its pathogenic cascade are now available.^{25,26} Antibodies against vascular endothelial growth factor (VEGF) uniquely offer a significant chance of increase in visual acuity to patients affected by neovascular AMD. Anti-VEGF therapy can provide long-term vision maintenance in more than 90% and substantial visual improvement in 25% to 40% of patients.^{27,28}

Monitoring response to therapy is one of the most important clinical uses of OCT. OCT can be used to quantify changes in central retinal thickness and volume, as well as subretinal fluid, which are parameters used in combination with visual acuity to analyze the response to therapy in several diseases, including neovascular AMD. Fung et al. used OCT to guide the treatment of neovascular AMD and demonstrated that OCT could detect the earliest signs of recurrent fluid in the macula after the ranibizumab injections were stopped.²⁹

OCT FINDINGS IN NEOVASCULAR AMD

Fluorescein angiography remains the gold standard for initial diagnosis of CNV, the defining characteristic of neovascular AMD. Correlation between OCT findings and leakage and staining on fluorescein angiography have been demonstrated using both time-domain OCT and SD-OCT systems.^{20,24} Small changes in the structure of the retinal layers and subretinal space can readily be noted, allowing the detection of morphological changes that may signal progression or regression of the lesions. As such, SD-OCT is a useful tool in diagnosing and monitoring anatomical changes associated with neovascular AMD.

Classic CNV on OCT can present as highly reflective fibrovascular tissue with irregular yet defined borders between the RPE and Bruch's membrane, or above the RPE (Fig. 2A).³⁰ Likewise, CNV may also present as a localized fusiform serous or fibrovascular PED (Fig. 2B).³¹ CNV not well defined by fluorescein angiography, or occult CNV, may present as RPE elevation from the underlying choroidal plane and may be composed of either serous or fibrovascular tissue (Fig. 3).^{6,31}

CNV, when active, is associated with presence of fluid, which appears on OCT as well circumscribed hyporeflective spaces that distort the surrounding retinal architecture. The fluid can accumulate in the subretinal or sub-RPE space or between all layers of the inner retina, and it can be quantitatively evaluated with OCT (Figs. 2 and 3).^{6,32} Recent studies show that SD-OCT is superior to time-domain OCT in detecting subretinal, sub-RPE, and intraretinal fluid, making it better for evaluation of CNV activity.³³

Freund et al. proposed a more refined classification of CNV that is not based on any single imaging modality but on information from a variety of imaging techniques, such as combined fluorescein angiography and SD-OCT, high-speed SD-OCT, and indocyanine green angiography, when necessary.¹² This new classification divides the neovascularization into three types and has the objectives to refine the treatment strategies and to provide a prognosis factor.

Type 1 neovascularization is characterized by vessels proliferating under the RPE. With fluorescein angiography it is described as occult or poorly defined CNV. In indocyanine green angiography it presents as a low-intensity hyperfluorescence. On OCT it appears as localized fusiform serous or fibrovascular PED (Figs. 2B and 3). The type 1 neovascularization usually presents a fairly mature neovascular tissue that may incompletely respond to anti-VEGF therapy.¹² The polypoidal choroidal vasculopathy is included in this classification as a variant of the type 1 neovascularization.

Type 2 neovascularization is characterized by the proliferation of the neovascular tissue above the RPE, in the subretinal space. With fluorescein angiography it is described as classic. It may be more difficult to identify on indocyanine green angiography due to the hyperfluorescence of the background choroidal circulation. SD-OCT localizes the vessels between the RPE and the photoreceptor outer segments (Fig. 2A). Disruption of the inner/outer segment photoreceptor junction and intraretinal cystic spaces is often observed. The type 2 vessels may present complete response to anti-VEGF therapy.¹²

Type 3 neovascularization, commonly referred to as retinal angiomatous proliferation, is characterized by intraretinal neovascularization and has a distinct presentation on OCT. Imaging characteristics include sub-RPE CNV with intraretinal angiomatous change along with subretinal neovascularization and cystic change. These changes have been demonstrated to correlate with clinical and angiographic findings and are hypothesized to be caused by aberrant retinal–choroidal anastomosis (Fig. 4).³⁴ Type 3 neovascularization appears to be sensitive to anti-VEGF therapy, early in its evolution.¹²

An additional feature of neovascular AMD is RPE tears or rips. They are known to occur spontaneously as a feature of the disease and as a result of therapy. On OCT, a tear in the RPE is characterized by a focal defect in the RPE with scrolling at the borders along with pleating of the adjacent continuous RPE (Fig. 5). RPE rips are associated with the presence of a domeshaped PED.³⁵

Additionally, end-stage AMD can be visualized as a disciform scar made up of hyperreflective tissue in the same location as the inciting CNV accompanied by retinal atrophy.⁶

ANATOMIC ASSESSMENT OF THERAPEUTIC RESPONSE

Currently, inhibition of VEGF-A is the first choice of therapy for neovascular AMD, which not only stabilizes but also improves visual acuity. The most effective preparations, bevacizumab (Avastin; Genentech Inc., South San Francisco, CA) or ranibizumab (Lucentis; Genentech Inc.), are recombinant monoclonal antibodies (Fab) that neutralize all biologically active forms of VEGF.²⁶ Two Phase III clinical trials (MARINA and ANCHOR) used ranibizumab for the treatment of CNV associated with neovascular AMD.^{27,28} In both of these studies, ranibizumab was administered every 4 weeks (fixed schedule) for up to 2 years without monthly imaging. Both trials demonstrated prevention of substantial vision loss (lost < 15 letters) in more than 90% of subjects. Additionally, approximately 30% to 40% of the subjects experienced substantial visual acuity gain (gain > 15 letters). Although these dramatic results have revolutionized the treatment of neovascular

AMD, the monthly treatment schedule used in the clinical trials has several drawbacks, including the high number of injections and the challenge of determining an end-point to treatment.

Consequently, to evaluate the effectiveness of less frequent ranibizumab treatment schedules on neovascular AMD, the PIER study³⁶ evaluated a reduced-frequency treatment schedule that consisted of intravitreal injection of ranibizumab once a month for the first 3 months followed by injections once every 3 months. A reduced chance of substantial vision loss was observed. However, the treatment schedule tested failed to demonstrate an increased chance of substantial vision gain compared with sham.

As such, the best criteria for re-treatment are uncertain. The strategies for treatment indication and particularly follow-up have to be adapted according to new treatment modalities. When considering re-treatment in neovascular AMD, fluorescein angiography was commonly used as an indicator of CNV activity; however, several reports have indicated inability to differentiate between leakage and staining and poor agreement in interpretation of fluorescein angiography in neovascular AMD between physicians, especially after treatment.^{20,37} Fluorescein angiography is also an invasive modality, rendering it not ideal for a monthly follow-up. Visual acuity alone depends on many factors, such as cataract progression. It is a psychophysical measurement with limited reliability.

By contrast, OCT offers many advantages: it is non-invasive and provides an objective measurement of retinal thickening and extravasated fluid. Further, OCT has been validated against fluorescein angiography, the gold standard, in the evaluation of retinal vascular leakage.^{20,23,24} OCT detects abnormalities, such as interstitial fluid, retinal cystoid abnormalities, and subretinal fluid, when fluorescein leakage from CNV is present. SD-OCT also frequently seems to detect abnormalities in the absence of fluorescein leakage from CNV. Khurana et al. confirmed that the abnormalities more frequently detected on SD-OCT seemed to correspond to 90% of cases with fluorescein leakage from CNV.²⁴ Additionally, studies have shown a correlation between retinal morphology on SD-OCT and visual function. For example, reduction in thickness of the neurosensory retina at the foveal center correlates with improvement in visual acuity.³⁸ Likewise, reduction of the size of subretinal tissue on OCT has been correlated with amelioration of contrast sensitivity.³⁹ Furthermore, disruption of the inner segment/outer segment junction on SD-OCT, which is an important indicator of photoreceptor integrity, has been correlated with irreversible reduction in visual function.^{23,40}

In contrast with previous clinical trials, the PrONTO study (Prospective OCT Imaging of Patients with Neovascular AMD Treated with Intra-Ocular Lucentis) included macular time-domain OCT features as part of the re-treatment criteria.²⁹ In this OCT-guided study, visual outcomes were similar to the results from the MARINA and ANCHOR clinical trial regimens, but the patients in the PrONTO study received an average of 9.9 injections over 24 months. Analysis of the study data after completion of the clinical trial demonstrated that OCT findings predicted the need for re-treatment based on features such as appearance of macular cysts or subretinal fluid, and these signs were thought to represent the earliest manifestations of recurrent CNV. Other OCT-guided studies using ranibizumab^{41,42} or bevacizumab⁴³ confirmed the visual outcomes reported by the PrONTO study using similar numbers of intravitreal injections.

These OCT-guided studies used time-domain OCT that has an axial resolution of less than 10 μm , with a relatively slow data-acquisition speed (400 A-scans/second). Recently developed SD-OCT devices offer improved image resolution of less than 3 to 7 μm with dramatically faster acquisition speeds (18,000 to 40,000 A-scan/second). Studies

demonstrated that SD-OCT provides more detailed views of the intraretinal cysts, intraretinal fluid, subretinal fluid, and subretinal pigment epithelium fluid when compared with time-domain OCT.²³ There is a correlation between retinal morphology on OCT and visual function.^{38,39} For these reasons, SD-OCT devices have higher and earlier detection rates of CNV activity. For an average patient, earlier detection means a significant gain of vision, which may be equivalent to or better than the gain achieved with most CNV treatments.⁴⁴

The incorporation of SD-OCT into clinical practice has improved decision-making ability in the treatment of neovascular AMD (Figs. 5 and 6). However, these instruments have not yet been validated in the context of anti-VEGF therapy. The Comparison of Age-related Macular Degeneration Treatments Trial will identify the best approach to anti-VEGF therapy (bevacizumab and ranibizumab) to be used as the standard of comparison for subsequent clinical trials for neovascular AMD. This trial has four arms: two with a fixed schedule for every 4 weeks and two with a variable dosing schedule. On the variable dosing arm, patients are evaluated monthly using visual acuity and time-domain OCT or SD-OCT images. Treatment in the follow-up will be driven by the presence or absence of fluid (subretinal, intraretinal, or sub-RPE) on the OCT. This study will identify whether there is any difference between anti-VEGF therapies and evaluate whether use of SD-OCT images can improve outcomes.

In future studies, photoreceptor anatomy may be more readily assessed and quantified by SD-OCT, and could become an important prognostic factor for patients undergoing treatment for neovascular AMD.⁴⁵ Three-dimensional rendering of retinal and intraretinal structures may enable more detailed assessment of CNV, facilitating the decision-making ability in the treatment of neovascular AMD.

LIMITATIONS AND FUTURE DIRECTIONS

OCT technology has been used since its inception to monitor and quantitatively analyze changes in neovascular AMD. The first generation OCT system, time-domain OCT, acquires images with an axial resolution of approximately 10 μm with an image acquisition speed of 400 Hz.⁴⁶ By comparison, SD-OCT has an axial resolution from 3 μm in commercially available machines to as low as 2 to 3 μm in prototypical systems with image acquisition speeds of up to 312.5 kHz (Fig. 7).⁴⁷⁻⁵⁰ As such, SD-OCT enables the visualization and quantification of the intraretinal layers, which is valuable in monitoring the progression of neovascular AMD.

In addition to having increased axial resolution, SD-OCT also has dramatically increased image acquisition speed: from 50 to 100 times faster than time-domain OCT.⁵¹ As such, it is possible to acquire three-dimensional data sets with reduced motion artifact.⁴⁸ Whereas time-domain OCT systems rely on radial scan patterns of the macula to detect changes in retinal thickness, which leads to a large amount of sampling error,⁵² SD-OCT enables high-speed volumetric imaging of the macula, which provides comprehensive three-dimensional tomographic and morphologic information.³² Additionally, with the three-dimensional OCT data sets it is possible to calculate the fibrovascular lesion volume, which can be used to monitor the CNV regression.⁴⁵

Further, segmentation software used by both time-domain OCT and SD-OCT systems to reconstruct retinal thickness maps has also improved.⁵³ Time-domain OCT has been shown to have errors in segmentation as much as 42.9% of the time.⁵⁴ There are fewer instances of software breakdown such as inner/outer retinal layer misidentification and artifacts such as inaccurate foveal thickness and off-center fixation with the SD-OCT systems compared to that of time-domain OCT. It was found that among patients with neovascular AMD, time-

domain OCT had an error rate of 55.56% when determining macular thickness, whereas SD-OCT systems had error rates ranging from 3.85% to 19.23% depending on the system.^{55,56} Keane et al. found the error rate in defining macular thickness to be as high as 57% in SD-OCT.⁵⁷ As such, there is room for improvement in the accuracy of OCT segmentation software as it is used in monitoring neovascular AMD.

One approach to improving reproducibility and accuracy of calculated retinal thickness has been to improve image quality through both hardware and software modifications. Two strategies in this vein include the use of eye tracking and image averaging. Eye tracking is a method by which a static fundus image is taken, usually with the aid of scanning laser ophthalmoscopy, to which a three-dimensional OCT image is co-localized during acquisition. This co-localization ensures that there is minimal motion artifact in the horizontal and vertical directions.^{58–61}

With regard to image averaging, inherent in OCT interferometric signal detection is a certain amount of speckle or noise in the signal. When multiple B-scans are averaged together, there is a reduction in the amount of speckle with a preservation of the amount of signal. As such, averaging multiple B-scans together results in increased definition of the retinal layers.⁶² This tool makes more detailed characterization of neovascular AMD possible. Some experimental technologies that seek to further address the limitations of SD-OCT include the use of swept-source OCT and functional technologies such as Doppler OCT and polarization-sensitive OCT.⁶³

Swept-source OCT uses a swept cavity laser instead of a superluminescent diode laser, which is found in most SD-OCT systems. The swept cavity laser can emit different frequencies of light at a high rate of change. Consequently, spectrometer and line scan cameras are no longer necessary for image detection as they are in SD-OCT. This hardware change leads to the advantages of higher image acquisition speed and decreased motion artifact.^{64,65}

Another promising technology, polarization-sensitive OCT, uses tissue birefringence to detect the health of the RPE. This may be helpful in diagnosis and monitoring of neovascular AMD in the future.⁶⁶ Additionally, Doppler OCT, which takes multiple data sets in succession, is able to detect flow in retinal vessels.⁶⁷ This technology holds promise in monitoring neovascular AMD, specifically in determining whether a neovascular lesion is active or inactive.

Acknowledgments

Supported in part by a Research to Prevent Blindness Challenge grant to the New England Eye Center/Department of Ophthalmology-Tufts University School of Medicine, NIH contracts RO1-EY11289-23, R01-EY13178-07, R01-EY013516-07, Air Force Office of Scientific Research FA9550-07-1-0101 and FA9550-07-1-0014.

Dr. Duker receives research support from Carl Zeiss Meditec, Inc., Optovue, Inc., and Topcon Medical Systems, Inc.

REFERENCES

1. Friedman DS, O'Colmain BJ, Munoz B, et al. Prevalence of age-related macular degeneration in the United States. *Arch Ophthalmol*. 2004; 122:564–572. [PubMed: 15078675]
2. Klein R, Klein BE, Linton KL. Prevalence of age-related maculopathy: The Beaver Dam Eye Study. *Ophthalmology*. 1992; 99:933–943. [PubMed: 1630784]
3. Thylefors B. A global initiative for the elimination of avoidable blindness. *Indian J Ophthalmol*. 1998; 46:129–130. [PubMed: 10085623]

4. Bressler NM, Bressler SB, Fine SL. Age-related macular degeneration. *Surv Ophthalmol.* 1988; 32:375–413. [PubMed: 2457955]
5. Votruba M, Gregor Z. Neovascular age-related macular degeneration: present and future treatment options. *Eye (Lond).* 2001; 15:424–429. [PubMed: 11450768]
6. Castro, LC. Exudative age-related macular degeneration. In: Huang, D.; Duker, JS.; Fujimoto, JG., et al., editors. *Imaging the Eye From Front to Back with RTVue Fourier-Domain Optical Coherence Tomography.* 1st ed. SLACK Incorporated; Thorofare, NJ: 2010. p. 137-153.
7. Macular Photocoagulation Study Group. Occult choroidal neovascularization: influence on visual outcome in patients with age-related macular degeneration. *Arch Ophthalmol.* 1996; 114:400–412. Erratum in: *Arch Ophthalmol.* 1996;114:1023. [PubMed: 8602776]
8. Macular Photocoagulation Study Group. Laser photocoagulation of subfoveal recurrent neovascular lesions in age-related macular degeneration: results of a randomized clinical trial. *Arch Ophthalmol.* 1991; 109:1232–1241. [PubMed: 1718251]
9. Macular Photocoagulation Study Group. Argon laser photocoagulation for neovascular maculopathy: five-year results from randomized clinical trials. *Arch Ophthalmol.* 1991; 109:1109–1114. Erratum in: *Arch Ophthalmol.* 1992;110:761. [PubMed: 1714270]
10. Bressler NM, Arnold J, Benchaboune M, et al. Verteporfin therapy of subfoveal choroidal neovascularization in patients with age-related macular degeneration: additional information regarding baseline lesion composition's impact on vision outcomes—TAP report No. 3. *Arch Ophthalmol.* 2002; 120:1443–1454. [PubMed: 12427056]
11. Yannuzzi LA, Slakter JS, Sorenson JA, et al. Digital indocyanine green videoangiography and choroidal neovascularization. *Retina.* 1992; 12:191–223. [PubMed: 1384094]
12. Freund KB, Zweifel SA, Engelbert M. Do we need a new classification for choroidal neovascularization in age-related macular degeneration? *Retina.* 2010; 30:1333–1349. [PubMed: 20924258]
13. Gass JD. Biomicroscopic and histopathologic considerations regarding the feasibility of surgical excision of subfoveal neovascular membranes. *Am J Ophthalmol.* 1994; 118:285–298. [PubMed: 7521987]
14. Grossniklaus HE, Green WR. Histopathologic and ultrastructural findings of surgically excised choroidal neovascularization. Submacular Surgery Trials Research Group. *Arch Ophthalmol.* 1998; 116:745–749. [PubMed: 9639442]
15. Freund KB, Zweifel SA, Engelbert M. Do we need a new classification for choroidal neovascularization in age-related macular degeneration? *Retina.* 2010; 30:1333–1349. Erratum in: *Retina.* 2011;31:208. [PubMed: 20924258]
16. Huang D, Swanson EA, Lin CP, et al. Optical coherence tomography. *Science.* 1991; 254:1178–1181. [PubMed: 1957169]
17. Sull AC, Vuong LN, Price LL, et al. Comparison of spectral/Fourier domain optical coherence tomography instruments for assessment of normal macular thickness. *Retina.* 2010; 30:235–245. [PubMed: 19952997]
18. Hee MR, Bauman CR, Puliafito CA, et al. Optical coherence tomography of age-related macular degeneration and choroidal neovascularization. *Ophthalmology.* 1996; 103:1260–1270. [PubMed: 8764797]
19. Coscas F, Coscas G, Souied E, Tick S, Soubrane G. Optical coherence tomography identification of occult choroidal neovascularization in age-related macular degeneration. *Am J Ophthalmol.* 2007; 144:592–599. [PubMed: 17698019]
20. Eter N, Spaide RF. Comparison of fluorescein angiography and optical coherence tomography for patients with choroidal neovascularization after photodynamic therapy. *Retina.* 2005; 25:691–696. [PubMed: 16141855]
21. de Boer JF, Cense B, Park BH, Pierce MC, Tearney GJ, Bouma BE. Improved signal-to-noise ratio in spectral-domain compared with time-domain optical coherence tomography. *Opt Lett.* 2003; 28:2067–2069. [PubMed: 14587817]
22. Leitgeb R, Hitzinger C, Fercher A. Performance of fourier domain vs. time domain optical coherence tomography. *Opt Express.* 2003; 11:889–894. [PubMed: 19461802]

23. Sayanagi K, Sharma S, Yamamoto T, Kaiser PK. Comparison of spectral-domain versus time-domain optical coherence tomography in management of age-related macular degeneration with ranibizumab. *Ophthalmology*. 2009; 116:947–955. [PubMed: 19232732]
24. Khurana RN, Dupas B, Bressler NM. Agreement of time-domain and spectral-domain optical coherence tomography with fluorescein leakage from choroidal neovascularization. *Ophthalmology*. 2010; 117:1376–1380. [PubMed: 20452027]
25. Ferrara N, Gerber HP, LeCouter J. The biology of VEGF and its receptors. *Nat Med*. 2003; 9:669–676. [PubMed: 12778165]
26. Chen Y, Wiesmann C, Fuh G, et al. Selection and analysis of an optimized anti-VEGF antibody: crystal structure of an affinity-matured Fab in complex with antigen. *J Mol Biol*. 1999; 293:865–881. [PubMed: 10543973]
27. Rosenfeld PJ, Brown DM, Heier JS, et al. Ranibizumab for neovascular age-related macular degeneration. *N Engl J Med*. 2006; 355:1419–1431. [PubMed: 17021318]
28. Brown DM, Kaiser PK, Michels M, et al. Ranibizumab versus verteporfin for neovascular age-related macular degeneration. *N Engl J Med*. 2006; 355:1432–1444. [PubMed: 17021319]
29. Fung AE, Lalwani GA, Rosenfeld PJ, et al. An optical coherence tomography-guided, variable dosing regimen with intravitreal ranibizumab (Lucentis) for neovascular age-related macular degeneration. *Am J Ophthalmol*. 2007; 143:566–583. [PubMed: 17386270]
30. Giovannini A, Amato GP, Mariotti C, Scassellati-Sforzolini B. OCT imaging of choroidal neovascularisation and its role in the determination of patients' eligibility for surgery. *Br J Ophthalmol*. 1999; 83:438–442. [PubMed: 10434866]
31. Ahlers C, Michels S, Beckendorf A, Birngruber R, Schmidt-Erfurth U. Three-dimensional imaging of pigment epithelial detachment in age-related macular degeneration using optical coherence tomography, retinal thickness analysis and topographic angiography. *Graefes Arch Clin Exp Ophthalmol*. 2006; 244:1233–1239. [PubMed: 16977431]
32. Chen Y, Vuong LN, Liu J, et al. Three-dimensional ultrahigh resolution optical coherence tomography imaging of age-related macular degeneration. *Opt Express*. 2009; 17:4046–4060. [PubMed: 19259245]
33. Cukras C, Wang YD, Meyerle CB, Forooghian F, Chew EY, Wong T. Optical coherence tomography-based decision making in exudative age-related macular degeneration: comparison of time- vs spectral-domain devices. *Eye (Lond)*. 2010; 24:775–783. [PubMed: 19696804]
34. Truong SN, Alam S, Zawadzki RJ, et al. High resolution Fourier-domain optical coherence tomography of retinal angiomatous proliferation. *Retina*. 2007; 27:915–925. [PubMed: 17891017]
35. Chang LK, Flaxel CJ, Lauer AK, Sarraf D. RPE tears after pegaptanib treatment in age-related macular degeneration. *Retina*. 2007; 27:857–863. [PubMed: 17891009]
36. Regillo CD, Brown DM, Abraham P, et al. Randomized, double-masked, sham-controlled trial of ranibizumab for neovascular age-related macular degeneration: PIER Study year 1. *Am J Ophthalmol*. 2008; 145:239–248. [PubMed: 18222192]
37. Friedman SM, Margo CE. Choroidal neovascular membranes: reproducibility of angiographic interpretation. *Am J Ophthalmol*. 2000; 130:839–841. [PubMed: 11124312]
38. Keane PA, Liakopoulos S, Chang KT, et al. Relationship between optical coherence tomography retinal parameters and visual acuity in neovascular age-related macular degeneration. *Ophthalmology*. 2008; 115:2206–2214. [PubMed: 18930551]
39. Keane PA, Patel PJ, Ouyang Y, et al. Effects of retinal morphology on contrast sensitivity and reading ability in neovascular age-related macular degeneration. *Invest Ophthalmol Vis Sci*. 2010; 51:5431–5437. [PubMed: 20554607]
40. Hayashi H, Yamashiro K, Tsujikawa A, Ota M, Otani A, Yoshimura N. Association between foveal photoreceptor integrity and visual outcome in neovascular age-related macular degeneration. *Am J Ophthalmol*. 2009; 148:83–89. [PubMed: 19327745]
41. Rothenbuehler SP, Waeber D, Brinkmann CK, Wolf S, Wolf-Schnurrbusch UE. Effects of ranibizumab in patients with subfoveal choroidal neovascularization attributable to age-related macular degeneration. *Am J Ophthalmol*. 2009; 147:831–837. [PubMed: 19217019]

42. Querques G, Azrya S, Martinelli D, et al. Ranibizumab for exudative age-related macular degeneration: 24-month outcomes from a single-centre institutional setting. *Br J Ophthalmol.* 2010; 94:292–296. [PubMed: 19951942]
43. Leydolt C, Michels S, Prager F, et al. Effect of intravitreal bevacizumab (Avastin) in neovascular age-related macular degeneration using a treatment regimen based on optical coherence tomography: 6- and 12-month results. *Acta Ophthalmol.* 2010; 88:594–600. [PubMed: 19485959]
44. Loewenstein A. The significance of early detection of age-related macular degeneration: Richard & Hinda Rosenthal Foundation lecture, The Macula Society 29th annual meeting. *Retina.* 2007; 27:873–878. [PubMed: 17891011]
45. Witkin AJ, Vuong LN, Srinivasan VJ, et al. High-speed ultrahigh resolution optical coherence tomography before and after ranibizumab for age-related macular degeneration. *Ophthalmology.* 2009; 116:956–963. [PubMed: 19410953]
46. Gabriele ML, Wollstein G, Ishikawa H, et al. Three dimensional optical coherence tomography imaging: advantages and advances. *Prog Retin Eye Res.* 2010; 29:556–579. [PubMed: 20542136]
47. Kagemann L, Ishikawa H, Wollstein G, Gabriele M, Schuman JS. Visualization of 3-D high speed ultrahigh resolution optical coherence tomographic data identifies structures visible in 2D frames. *Opt Express.* 2009; 17:4208–4220. [PubMed: 19259256]
48. Wojtkowski M, Srinivasan V, Fujimoto JG, et al. Three-dimensional retinal imaging with high-speed ultrahigh-resolution optical coherence tomography. *Ophthalmology.* 2005; 112:1734–1746. [PubMed: 16140383]
49. Potsaid B, Gorczynska I, Srinivasan VJ, et al. Ultrahigh speed spectral/Fourier domain OCT ophthalmic imaging at 70,000 to 312,500 axial scans per second. *Opt Express.* 2008; 16:15149–15169. [PubMed: 18795054]
50. Ko TH, Fujimoto JG, Schuman JS, et al. Comparison of ultrahigh- and standard-resolution optical coherence tomography for imaging macular pathology. *Ophthalmology.* 2005; 112:192.
51. Kaluzny JJ, Wojtkowski M, Sikorski BL, et al. Analysis of the outer retina reconstructed by high-resolution, three-dimensional spectral domain optical coherence tomography. *Ophthalmic Surg Lasers Imaging.* 2009; 40:102–108. [PubMed: 19320297]
52. Alam S, Zawadzki RJ, Choi S, et al. Clinical application of rapid serial fourier-domain optical coherence tomography for macular imaging. *Ophthalmology.* 2006; 113:1425–1431. [PubMed: 16766031]
53. Ahlers C, Simader C, Geitzenauer W, et al. Automatic segmentation in three-dimensional analysis of fibrovascular pigmentepithelial detachment using high-definition optical coherence tomography. *Br J Ophthalmol.* 2008; 92:197–203. [PubMed: 17965102]
54. Krebs I, Haas P, Zeiler F, Binder S. Optical coherence tomography: limits of the retinal-mapping program in age-related macular degeneration. *Br J Ophthalmol.* 2008; 92:933–935. [PubMed: 18577644]
55. Ho J, Sull AC, Vuong LN, et al. Assessment of artifacts and reproducibility across spectral- and time-domain optical coherence tomography devices. *Ophthalmology.* 2009; 116:1960–1970. [PubMed: 19592109]
56. Giani A, Cigada M, Esmaili DD, et al. Artifacts in automatic retinal segmentation using different optical coherence tomography instruments. *Retina.* 2010; 30:607–616. [PubMed: 20094011]
57. Keane PA, Mand PS, Liakopoulos S, Walsh AC, Sassa SR. Accuracy of retinal thickness measurements obtained with Cirrus optical coherence tomography. *Br J Ophthalmol.* 2009; 93:1461–1467. [PubMed: 19574239]
58. Hammer D, Ferguson RD, Iftimia N, et al. Advanced scanning methods with tracking optical coherence tomography. *Opt Express.* 2005; 13:7937–7947. [PubMed: 19498823]
59. Hammer DX, Ferguson RD, Magill JC, et al. Active retinal tracker for clinical optical coherence tomography systems. *J Biomed Opt.* 2005; 10:024038. [PubMed: 15910111]
60. Ferguson RD, Hammer DX, Paunescu LA, Beaton S, Schuman JS. Tracking optical coherence tomography. *Opt Lett.* 2004; 29:2139–2141. [PubMed: 15460882]
61. Brinkmann CK, Wolf S, Wolf-Schnurbusch UE. Multimodal imaging in macular diagnostics: combined OCT-SLO improves therapeutical monitoring. *Graefes Arch Clin Exp Ophthalmol.* 2008; 246:9–16. [PubMed: 17674015]

62. Sakamoto A, Hangai M, Yoshimura N. Spectral-domain optical coherence tomography with multiple B-scan averaging for enhanced imaging of retinal diseases. *Ophthalmology*. 2008; 115:1071–1078. [PubMed: 18061270]
63. Drexler W, Fujimoto JG. State-of-the-art retinal optical coherence tomography. *Prog Retin Eye Res*. 2008; 27:45–88. [PubMed: 18036865]
64. Huber R, Adler DC, Srinivasan VJ, Fujimoto JG. Fourier domain mode locking at 1050 nm for ultra-high-speed optical coherence tomography of the human retina at 236,000 axial scans per second. *Opt Lett*. 2007; 32:2049–2051. [PubMed: 17632639]
65. Huber R, Wojtkowski M, Fujimoto JG. Fourier Domain Mode Locking (FDML): A new laser operating regime and applications for optical coherence tomography. *Opt Express*. 2006; 14:3225–3237. [PubMed: 19516464]
66. Ahlers C, Gotzinger E, Pircher M, et al. Imaging of the retinal pigment epithelium in age-related macular degeneration using polarization-sensitive optical coherence tomography. *Invest Ophthalmol Vis Sci*. 2010; 51:2149–2157. [PubMed: 19797228]
67. Leitgeb RA, Schmetterer L, Hitzenberger CK, et al. Real-time measurement of in vitro flow by Fourier-domain color Doppler optical coherence tomography. *Opt Lett*. 2004; 29:171–173. [PubMed: 14744000]

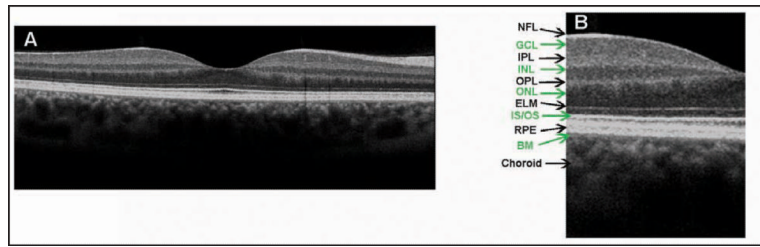


Figure 1.

(A) Cross-sectional Cirrus HD-OCT (Carl Zeiss Meditec, Inc., Dublin, CA) image of the normal macula. (B) An enlargement of the image demonstrates the ability to visualize intraretinal layers that can be correlated with intraretinal anatomy: nerve fiber layer (NFL), ganglion cell layer (GCL), inner plexiform layer (IPL), inner nuclear layer (INL), outer plexiform layer (OPL), outer nuclear layer (ONL), external limiting membrane (ELM), junction of inner and outer photoreceptor segments (IS/OS), retinal pigment epithelium (RPE), and Bruch's membrane (BM).

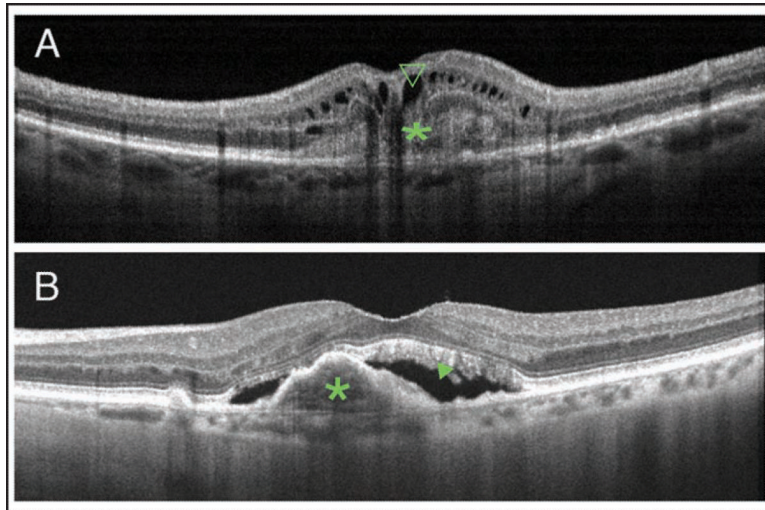


Figure 2.

Cross-sectional optical coherence tomography (OCT) images showing different types of choroidal neovascularization (CNV). (A) Cross-sectional image captured by RTVue (Optovue, Inc., Fremont, CA) showing a classic CNV, type 2 neovascularization, delineated as a nonuniform moderately hyperreflective formation above the RPE (green *) and the presence of intraretinal cysts (green open arrowhead). (B) Cross-sectional image captured by Heidelberg Spectralis HRA+OCT (Heidelberg Engineering, Heidelberg, Germany) showing a fibrovascular pigment epithelial detachment, type 1 neovascularization (green *), and the presence of subretinal fluid (green closed arrowhead).

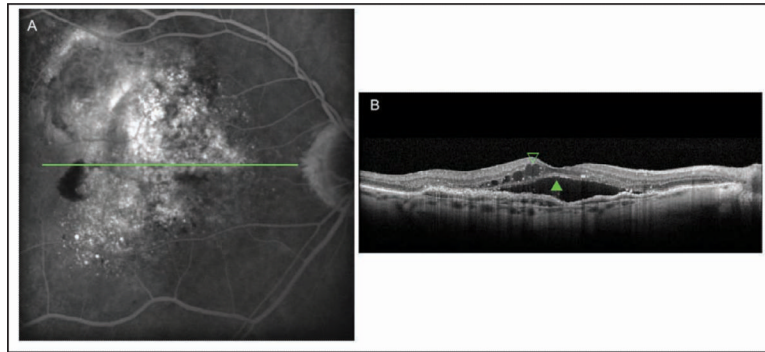


Figure 3. Occult choroidal neovascularization membrane. (A) The fluorescein angiogram performed in Heidelberg Spectralis HRA+OCT (Heidelberg Engineering, Heidelberg, Germany) showed a speckled hyperfluorescence with dye pooled in the subretinal space on the late phase of the examination. (B) Cross-sectional image of Spectralis device depicted the thickened retinal pigment epithelium raised by non-uniform moderate hyperreflective formation with the presence of subretinal fluid (green closed arrowhead) and intraretinal fluid (green open arrowhead).

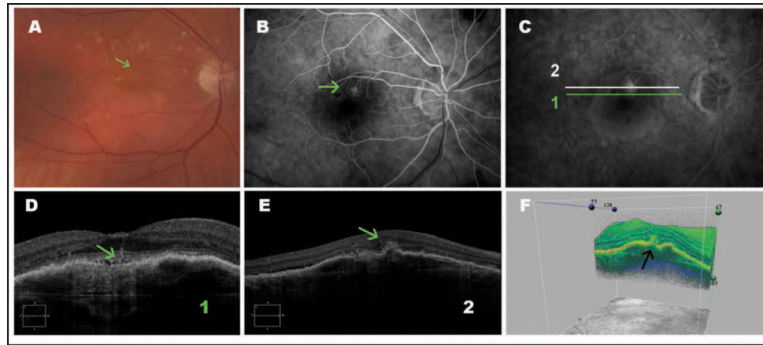


Figure 4.

Type 3 neovascularization (retinal angiomatous proliferation). (A) Color photography showing intraretinal hemorrhage (green arrow). (B and C) Fluorescein angiograms show poorly defined hyperfluorescence typical of retinal angiomatous proliferation (green arrow). (D) An enlarged cross-sectional Cirrus HD-OCT (Carl Zeiss Meditec, Inc., Dublin, CA) image showing a pigment epithelium detachment and a vessel penetrating the retina (green arrow). (E) Cross-sectional Cirrus HD-OCT image showing a pigment epithelial detachment, a hyperreflective material (green arrow) that can be the neovascular tissue, in the outer retina layers. (F) Three-dimensional Cirrus HD-OCT image showing a hyperreflective material in the outer retina layers (black arrow).

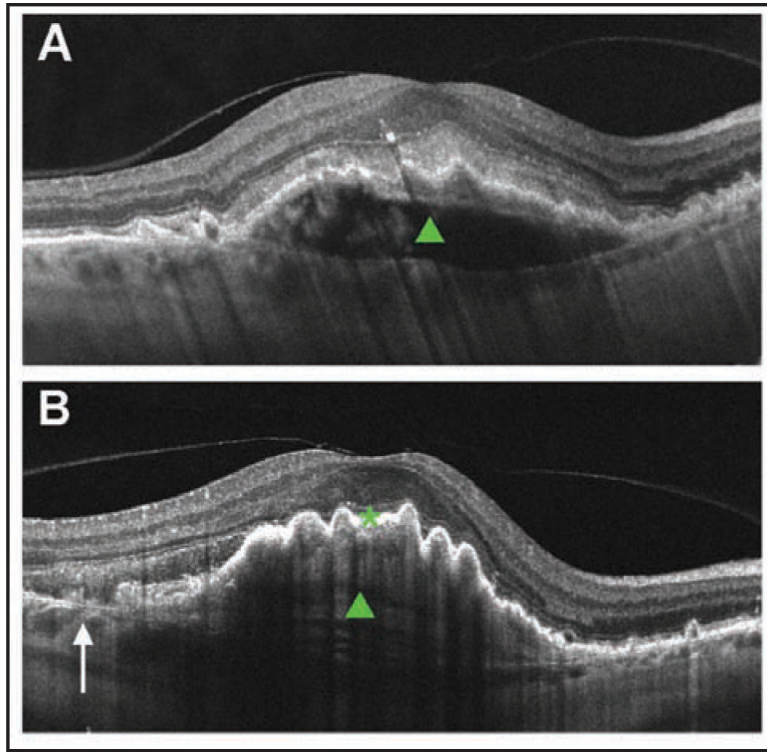


Figure 5. Cross-sectional Cirrus HD-OCT (Carl Zeiss Meditec, Inc., Dublin, CA) image of a fibrovascular pigment epithelium detachment (PED) before and after retinal pigment epithelium (RPE) rip. (A) Cross-sectional image before rip. Note dome-shaped PED (green closed arrowhead) and intact RPE layer. (B) Cross-sectional image after rip. Arrow denotes discontinuity of the RPE layer. Note RPE scrolling at the edge of the RPE defect and pleating RPE over the PED (green closed arrowhead).

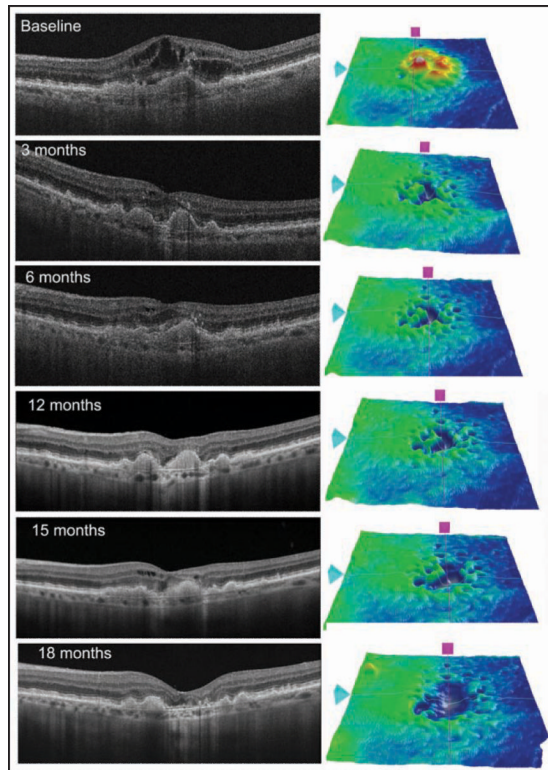


Figure 6.

Sequential spectral-domain optical coherence tomography (OCT) scans of a 75-year-old woman with subfoveal choroidal neovascularization (CNV). A baseline scan depicted an elevation of the retinal pigment epithelium (RPE) layer, a localized fusiform thickening and duplication of the highly reflective external band (RPE/choriocapillaris complex), and intraretinal fluid corresponding to CNV. The patient was treated with intravitreal injection of ranibizumab at baseline, month 1, and month 2. Three months after the first injection, the OCT scan demonstrated improvement of macular architecture with mild intraretinal fluid. Additionally, the thickness map showed a significant decrease in the retinal thickness at the macular region. Between 3 and 12 months after treatment, three injections were administered due to the presence of discrete intraretinal fluid. It is important to note the better resolution of the 12-month scan due to image oversampling. The improvement in the resolution leads to a better visualization of retinal layers and it is possible to note the inner/outer segment junction interruption. At 15 months from the first injection, the patient presented intraretinal fluid and was treated with intravitreal ranibizumab. At 18 months of follow-up, no fluid was detected in the macular area, but the thickness map showed a diffuse thinning.

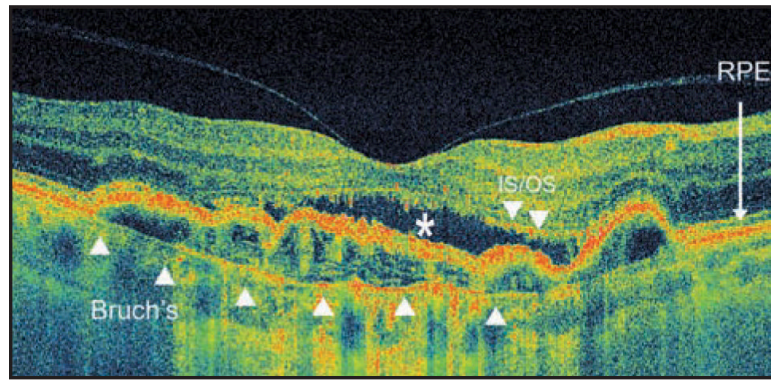


Figure 7. High pixel density high-speed ultra-high-resolution optical coherence tomography image from occult choroidal neovascularization. Note discontinuity of the inner/outer segment (IS/OS) junction line, subretinal fluid (white *), and pigment epithelium detachment. Bruch's membrane is demonstrated with the white arrowheads. RPE = retinal pigment epithelium.